ASSIMILATING THE WINDSAT WINDS IN THE NCEP GLOBAL DATA ASSIMILATION SYSTEM AND DETERMING THE FORECAST IMPACT FROM A TWO-SEASON STUDY

Li Bi [1,3] James A. Jung [1,2] John F. Le Marshall [4,1]

[1] Cooperative Institute for Meteorological Satellite Studies, Univ. of WI-Madison
[2] Joint Center for Satellite Data Assimilation, Camp Springs, MD
[3] Atmospheric and Oceanic Sciences, Univ. of WI-Madison
[4]Centre for Australian Weather and Climate Research (CAWCR), Australia

ABSTRACT

The results from a two-season impact study assimilating US Naval Research Laboratories (NRL) WindSat Environmental Data Records (EDRs) surface winds into the National Centers for Environmental Prediction (NCEP) global forecast system are presented. Comparisons between the control forecast (conventional database including QuikSCAT winds) and the WindSat experiment (control database with QuikSCAT winds plus the NRL WindSat winds) are made. The impact of assimilating these winds is measured by calculating anomaly correlation scores and geographic Forecast Impacts. Comparisons of assimilating these winds to the control experiment will be presented. Quality control procedures pertinent to the NCEP global model will also be discussed.

The results in this study demonstrate that assimilating the surface winds from the WindSat sensor on the CORIOLIS satellite show improvement in low level wind and temperature forecasts, especially in the tropics.

1. INTRODUCTION

Sea surface wind vectors have been estimated using active remote sensing instruments, such as QuikSCAT (Yu and McPherson 1984), and have been shown to have a positive impact on forecasts. Passive polarimetric microwave radiometry is being introduced as an alternative vector wind measurement approach to the active remote sensing approach of QuikSCAT and other instruments. As a result WindSat, a space-based multi-frequency polarimetric microwave radiometer (Gaiser et al., 2004), was developed by the Naval Research Laboratory for the U.S. Navy and the National Polar-orbiting Operational Environmental Satellite System (NPOESS) Integrated Program Office (IPO). The projected capabilities of the WindSat mission are to demonstrate spaceborne remote sensing of ocean surface wind vectors (speed and direction). Wind direction measurement with polarimetric instruments, which sense the polarity of light, also demonstrate how ocean surface properties change with wind and boundary layer conditions. WindSat will aid with forecasting short-term weather, issuing timely weather warnings and gathering general climate data. WindSat wind vectors have been proven to have a positive impact on forecasts in the Southern Hemisphere (Le Marshall et al, 2006).

2. BACKGROUND

2.1 WindSat

The WindSat radiometer on the CORIOLIS satellite has polarimetric channels at 10.7, 18.7 and 37.0 GHz and dual-polarization (vertical and horizontal) channels at 6.8 and 23.8 GHz. These provide information related to surface wind vectors as well as sea surface temperature, atmospheric water vapor, integrated cloud liquid water and rain rate over the ocean. Measurements of the modified stokes vector, which includes the vertical and horizontal polarizations and the third and fourth stokes parameters, provides sufficient information to retrieve the ocean wind vector (Bettenhausen et al., 2006). The 6.8GHz dual-polarized channel is more sensitive to sea surface temperature (SST) than to winds and is used to

determine effects due to variations in SST. Similarly, the 23.8GHz dual-polarized channel is highly sensitive to atmospheric water vapor. Consequently, measurements at 23.8 GHz help determine the effects of atmospheric attenuation on radiation from the ocean surface.

Wind roughening the surface of the ocean causes an increase in the brightness temperature of the microwave radiation emitted from the water's surface. From the brightness temperature measured by satellite radiometers, wind speed and direction can be retrieved. The Navy's ocean surface wind vectors used in this study have been determined using a non-linear iterative optimal estimation method. Details of the scheme which uses a one layer atmospheric model and a sea surface emissivity model is found in Bettenhausen et al., (2006). The Naval Research Laboratory (NRL) WindSat Version 2 wind vector retrieval algorithm has been used in this study (Bettenhausen et al., 2006). The Environmental Data Records (EDRs) generated by this scheme have been put into Binary Universal Form for the Representation of meteorological data (BUFR) format at NCEP for operational use.

2.2 Global Data Assimilation System

For these experiments, the NCEP Global Data Assimilation/Forecast System (GDAS/GFS) was used with a horizontal resolution of 382 spectral triangular waves (T382) and 64 vertical layers. The most recent information about the GFS atmospheric model is available from NCEP (or online at http://www.emc.ncep.noaa.gov/officenotes/newernotes/on442.pgf). The analysis scheme is a three-dimensional variational data assimilation (3DVAR) scheme and is referred to as the Gridpoint Statistical Interpolation (GSI) (Derber et al. 1991; Derber et al. 2003).

3. EXPERIMENTAL DESIGN

The complete NCEP operational database of conventional and satellite data has been used, including the real-time data cut-off constraints for the early and late assimilation cycles produced at NCEP. The satellite observations used in this work include operational Advanced Television Infrared Observation Satellite (TIROS-N) (NOAA 2000), Operational Vertical Sounder (TOVS) (Smith et al. 1979) radiances from the High Resolution Infrared Radiation Sounder (HIRS), the Microwave Sounding Unit (MSU) (Spencer and Christy 1990), the Advanced Microwave Sounding Unit (AMSU-A and AMSU-B) sensors (NOAA 2005), ozone information from the Solar Backscatter Ultraviolet (SBUV) sensors (Miller et al. 1997); Defense Meteorological Satellite Program (DMSP) Special Sensor Microwave Imager (SSM/I) surface wind speed (Alishouse et al. 1990); derived surface winds from Quikscat (Yu and McPherson 1984); atmospheric motion vectors from geostationary satellites (Velden et al. 1997; Menzel et al. 1998). The conventional data used includes rawinsonde temperature, relative humidity and wind, aircraft observations of wind and temperature; land surface reports of surface pressure; and oceanic reports of surface pressure, temperature, horizontal wind and specific humidity. Keyser (2001a, 2001b, 2003) provides an overview of data types provided to NCEP on a daily basis and used operationally for the experiments of this study.

Data thinning was achieved using a similar technique to that used operationally for QuikSCAT wind vectors, namely using super-observations. Tests were run to determine whether one degree or one- half degree latitude, longitude averaging boxes were more effective and it was found that the one degree boxes gave the best forecast result. Operational superobing is applied to the Navy's retrieved winds for each grid box. The two season time period studied is from 15 September to 30 October, 2006 and from 15 February to 30 March, 2007. A gross error check was also constructed for the data.

Most of the Quality Control (QC) of the WindSat data was accomplished in the retrieval process. Observations that fail the retrieval process or are flagged for rain, land, sun glint, RFI (Radio Frequency Interference) or sea ice contamination are omitted. Additional quality control procedures were added within GDAS/GFS. Observations not within +/- 3 hours of the synoptic time and observations near coasts were rejected before superobing. If the absolute value of the superobed wind component differs from the corresponding background wind by more than $6ms^{-1}$ or the wind was not between $4ms^{-1}$ and $20ms^{-1}$ they were removed.

After finalizing the quality control and data thinning, assimilation experiments were conducted to test the utility of the WindSat data for global numerical prediction. The Control contained all the operational data used during the period and included all of the real time data cutoff requirements. For this paper, forecast impact comparisons will be presented between a system assimilating the WindSat data and a Control experiment.

Several diagnostics were performed using the Control and WindSat experiment analyses and forecasts. The anomaly correlation statistics were performed using the traditional NCEP algorithms (NWS 2006) which are commonly used by Numerical Weather Prediction (NWP) centers world wide. The computation of all anomaly correlations for forecasts produced by the GFS are completed using code developed and maintained at NCEP. NCEP (NWS 2006) provides a description of the method of computation while Lahoz (1999) presents an overall description of what the anomaly correlation is typically used for. The NCEP/NCAR reanalysis fields (Kistler 2001) are used for the climate component of the anomaly correlations. To calculate anomaly correlations the output grids from the control and both experiments were reduced to a 2.5^{o} by 2.5^{o} horizontal resolution using the GFS post processor. The fields being evaluated are truncated to only include spectral wave numbers 1 through 20. They are also limited to the zonal bands of 20^{o}-80° in each Hemisphere and a tropical belt within 20° of the equator (20°N to 20°S).

In addition to the anomaly correlation, another diagnostic used here is the geographic distribution of forecast impact (FI) explained in Zapotocny et al. (2005) and Zapotocny et al. (2007). For this assimilation and impact study, a series of two-dimensional FI results are shown at different levels. The geographic distribution of FI for a specific level is calculated using:

$$FI(x,y) = 100\mathrm{X}\left\{\left(\sqrt{\frac{\sum_{i=1}^{N}(\mathrm{C}i-\mathrm{A}i)^2}{\mathrm{N}}}-\sqrt{\frac{\sum_{i=1}^{N}(\mathrm{E}i-\mathrm{A}i)^2}{\mathrm{N}}}\right)\Bigg/\sqrt{\frac{\sum_{i=1}^{N}(\mathrm{C}i-\mathrm{A}i)^2}{\mathrm{N}}}\right\}$$

The variables *C* and *E* are the control and experiment forecasts, respectively. The variable *A* is the GDAS experiment analysis containing all data types, which is valid at the same time as for forecasts. *N* is the number of diagnostic days.

Another diagnostic used here is the area weighted Root Mean Square Error (RMS) calculation discussed by Zapotocny et al. (2007). The area weighted RMS calculation accounts for the reduction in area as for grid boxes approach the poles.

4. RESULTS

The impact of assimilating the WindSat data on the quality of forecasts made by the GFS for two time periods have been explored in detail. The first time period covers 15 September to 31 October 2006, the second covers 15 February to 30 March 2007. The selection of these time periods enables the diagnostics to sample two seasons in each hemisphere. The fields diagnosed in this paper consist of geopotential heights, temperature, and wind speed. Underground grid points on isobaric surfaces intersecting the earth's surface are not included in the evaluations.

Figure 1 displays a comparison of the standard deviation of observation minus background and observation minus analysis by WindSat wind speed bins. Panel (a) shows the results from October 2006 and panel (b) shows the results from March 2007. There are large standard deviations for wind speed greater than $20ms^{-1}$.

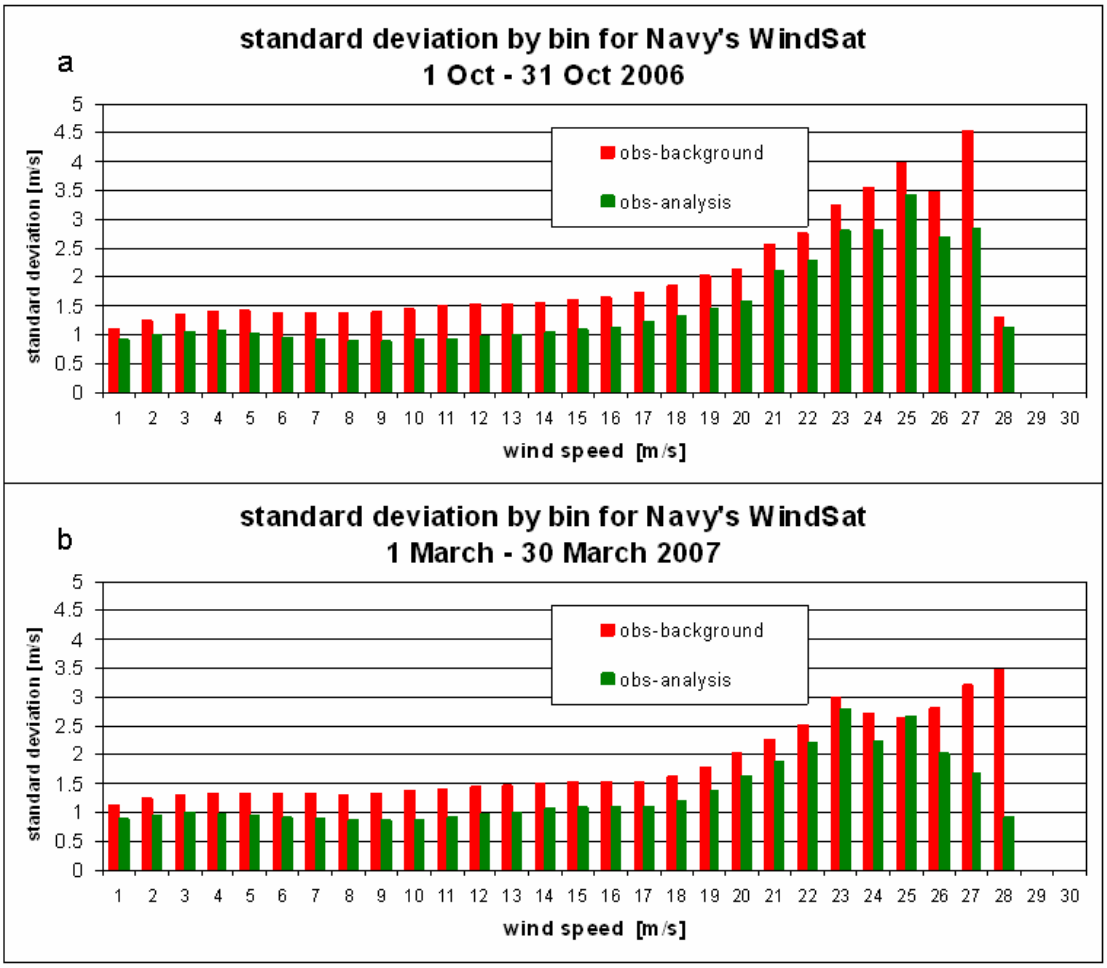

Figure 1. **Comparison of the standard deviation of observation minus background and observation minus analysis by bins for WindSat wind speed bins from WindSat runs using WindSat data. The top panel shows the results from 1 Oct – 31 Oct 2006 and the bottom panel shows the results from 1 March – 30 March 2007**

Figure 2 presents a comparison of the wind speed histogram by wind speed bins for WindSat assimilation runs. Panel (a) shows the results for October 2006 and panel (b) shows the results from March 2007. The blue curve shows the observation minus background and green curves represents the observation minus analysis. The observation minus background histograms are skewed to the right for both seasons which suggests a small positive bias for WindSat wind speed.

The Anomaly Correlation (AC) comparisons for mid-latitudes of 1000 and 500 hPa are presented in Figure 3. Panel (a) are the October 2006 and panel (b) are the March 2007 comparisons. The anomaly correlations at 500hPa at five days improvement in the Northern Hemisphere for both seasons as shown.

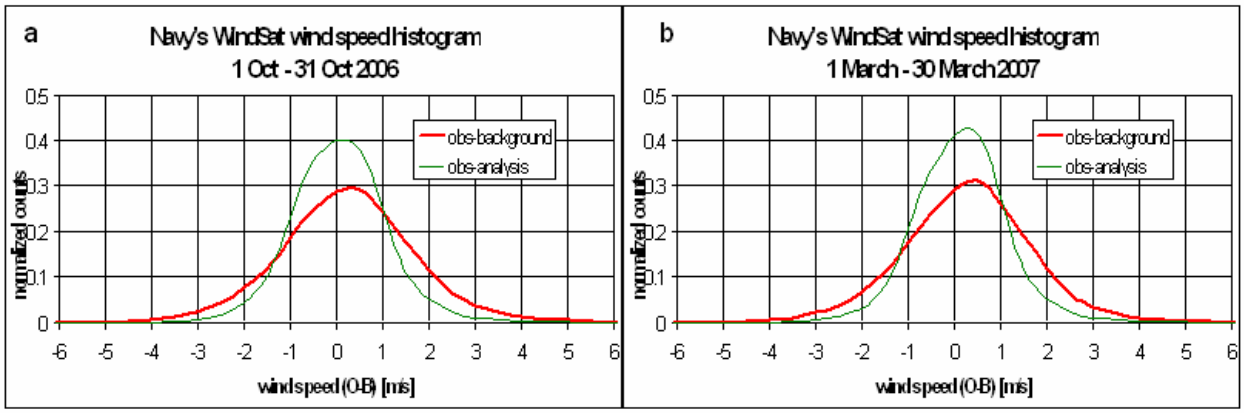

Figure 2. **Comparison of the wind speed histogram for WindSat from WindSat runs using WindSat data. The left panel shows the results from 1 Oct – 31 Oct 2006 and the right panel shows the results from 1 March – 30 March 2007.**

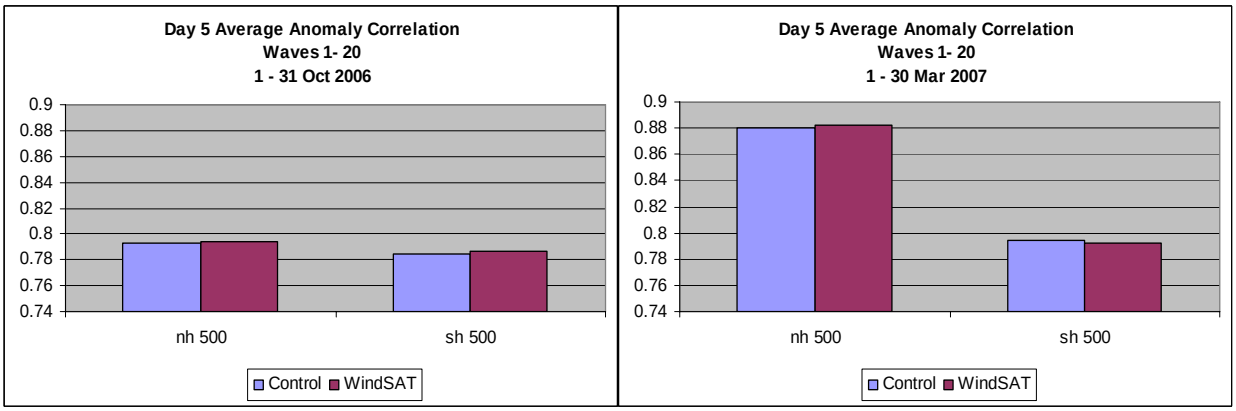

Figure 3. **Anomaly correlation bar charts in the region 20°-80° at day 5 for 500 and 1000 hPa geopotential height for each Hemisphere and season. The control simulation is shown in blue, while the WindSat experiment is shown in red. The left panel shows the result from 1-31 Oct 2006. The right panel shows the result from 1-30 March 2007. For all panels the results have been truncated to only show waves 1 - 20.**

Figure 4 displays geographic distributions of Forecast Impact determined using (1). Wind speed averaged over October 2006 at 10m level at forecast hours 6, 12, 24 and 48 are shown in panels a-d respectively, and March 2007 in panels e-h respectively. The range of FI is from -50 to 100. The 10m level is the level which is closest to where the WindSat wind observations are added to the assimilation system. The 6-h results (Fig. 4a) show the largest forecast impact in Africa, western Pacific, South America and Australia. By 12 hour (Fig. 4b), the FIs in western Pacific reduced, with the largest FI still realized over Africa, Australia and South America. The FIs are generally small by 24 hour (Fig. 4c) and become mostly neutral by 48 hours (Fig. 4d). Figure 4e-h presents the March 2007 WindSat 10m wind speed FIs at forecast hours 6, 12, 24, and 48 respectively. Consistent with the results in October, large positive forecast impacts are seen over Africa, Australia and South America at 6 hours (Fig. 4e), except over the western Pacific. By 12 hours (Fig. 4f), the largest impacts are only still found over Africa. Again, the FIs are generally small by 24 hours (Fig. 4g) and become mostly neutral by 48 hours (Fig. 4h).

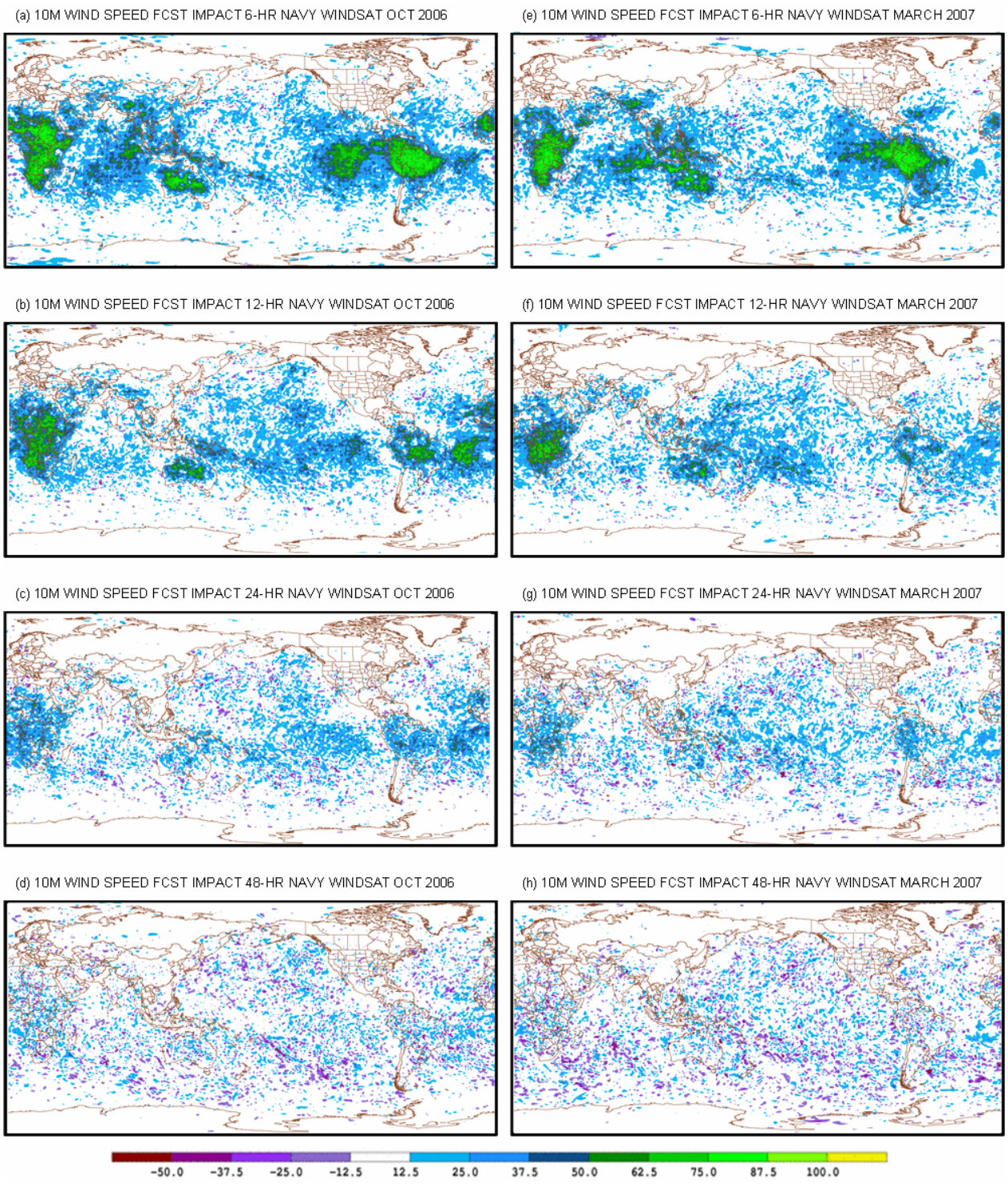

***Figure 4*. Geographic distribution of forecast impact from 1 October to 31 October for wind speed at 10m for WindSat retrieved winds at forecast hours (a) 6, (b) 12, (c) 24, and (d) 48 and from 1 March to 30 March at forecast hours (e) 6, (f) 12, (g) 24, and (h) 48. The range of forecast impact is from -50 to +100.**

Figure 5 presents vertical time series of the temporally and zonally averaged forecast impacts from both of the two season forecast impact experiments. Forecast impacts in the wind speed, and temperature fields are shown for each seasonal time window. Inspection of the plots reveals that the largest impacts are around the 500hPa level. Large FIs are also shows at 100hPa. Similar FI patterns are found for both seasons (Fig. 5a and c). Figure 5b and d present the October 2006 temperature

vertical time series FI. There are also two large temperature FIs shown at 500hPa and 100hPa for both seasons, similar to the wind speed. All four panels display a systematic decrease of FI with time. A final point about the vertical time series of the zonally and temporally averaged forecast impact results is that the 6-h temporal resolution of the GFS archive used for these experiments is inadequate to resolve the rapid decrease in forecast impact that occurs in the first 12 h of these simulations.

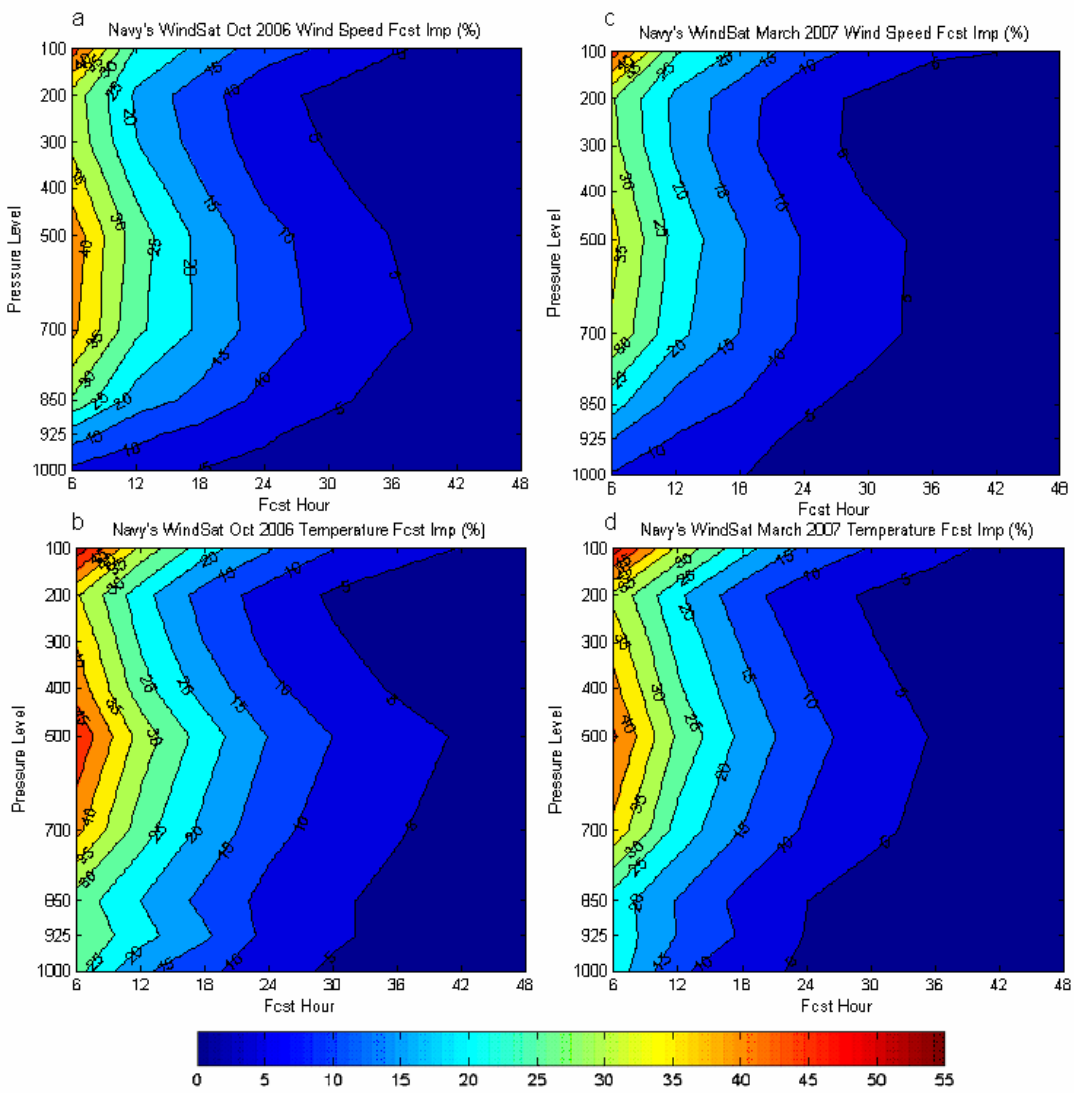

***Figure 5*. Cross sections of October 2006 WindSat forecast impact (%) to (a) wind speed, (b) temperature and March 2007 WindSat forecast impact to (c) wind speed and (d) temperature as a function of pressure (hPa) and forecast time (hr) for the entire globe. The colors have a uniform contour interval of 5%.**

5. SUMMARY

The WindSat data impact experiments for two 45-day periods in September-October 2006 and February – March 2007 have been completed using the NCEP GDAS. The anomaly correlation show neutral to modest positive impacts at mid- latitudes. Positive Forecast Impacts occurred in the wind, temperature and height fields (height fields not shown). The greatest Forecast Impacts occurred in the tropics and at 500 hPa. It was also found in this study that positive Forecast Impacts are noted at all levels of the GFS through 48 hours.

6. ACKOWLEDGEMENTS

The authors wish to thank Dr. Tom Zapotocny for leading WindSat project at UW. The authors also wish to thank Prof. Michael Morgan (UW-AOS) for local computer resources and Stephen Lord (NCEP) for use of the GFS/GDAS, computer resources and their tape archive. The authors wish to acknowledge John Derber and Lars Peter Riishojgaard for giving insightful advice. Thanks are also due to Peter Gaiser and Mike Bettenhausen for providing WindSat data, and Dennis Keyser and Stacie Bender for collecting and processing the various WindSat data streams. This research was supported under NOAA grant NA07EC0676 which supports JCSDA activities.

7. REFERENCES

Alishouse, J. C., S. Snyder, J. Vongsathorn, and R. R. Ferraro, 1990: Determination of oceanic total precipitable water from the SSM/I. *IEEE Trans. Geosci. Remote Sens*., **28**, 811-816.

Bettenhausen, M.H., Smith, C.K., Bevilacqua, R.M., Wang, N., Gaiser, P.W., and S. Cox, 2006: A Non-linear Optimization Algorithm for Wind sat Wind Vector Retrievals. *IEEE Trans. Geosci. Remote Sens.,* **44**, 597-610.

Derber, J. C., D. F. Parrish, and S. J. Lord, 1991:
The New Global Operational Analysis System at the National Meteorological Center. *Wea. Forecasting*, **6**, 538-547.

Derber , J. C., Van Delst, P., Su, X. J., Li, X., Okamoto, K. and Treadon, R. 2003: Enhanced use of radiance data in the NCEP data assimilation system.
Proceedings of the 13th International TOVS Study Conference. Ste. Adele, Canada, 20 October – 4 November, 2003.

Gaiser, P.W., St. Germain , K.M., Twarog, E.M., Poe, G.A., Purdy, W., Richardson, D., Grossman, W., Jones, W.L., Spencer, D., Golba, G., Cleveland, J., Choy, L., Bevilacqua, R.M., and P.S. Chang, 2004: The WindSat spaceborne polarimetric microwave radiometer: Sensor description and early orbit performance. *IEEE Trans. Geosci. Remote Sens.,* **42**, 2347-2361.

Lahoz, W. A., 1999: Predictive Skill of the UKMO Unified Model in the Lower Stratosphere. *Quart. J. Roy. Meteor. Soc*., **125**, 2205-2238.

Le Marshall, J., Bi, L., Jung, J., Zapotocny, T. and Morgan, M. 2006. WindSat Polarimetric Microwave Observations Improve Southern Hemisphere Numerical Weather Prediction**.** *Aust. Meteor. Mag*. **56,** 35-40.

Keyser, D., cited 2001a: Code table for PREPBUFR report types used by the ETA/3DVAR. [Available online from http://www.emc.ncep.noaa.gov/mmb/papers/keyser/prepbufr.doc/table_4.htm.]

_____, cited 2001b: Summary of the current NCEP analysis system usage of data types that do not pass through PREPBUFR processing. [Available online from http://www.emc.ncep.noaa.gov/mmb/papers/keyser/prepbufr.doc/table_19.htm.]

_____, cited 2003: Observational data processing at NCEP. [Available online from http://www.emc.ncep.noaa.gov/mmb/papers/keyser/data_processing/.]

Kistler, R., E. Kalnay, W. Collins, S. Saha, G. Withe, J. Woollen, M. Chelliah, W. Ebisuzaki, M. Kanamitsu, V. Kousky, H. Van den Dool, R. Jenne and M. Fiorino, 2001: The NCEP-NCAR 50-Year Reanalysis: Monthly Means CD-ROM and Documentation. *Bull. Amer. Meteor. Soc*, **82**, 247-267.

Menzel, W. P., F. C. Holt, T. J. Schmit, R. M. Aune, A. J. Schreiner, G. S. Wade, and D. G. Gray, 1998: Application of GOES-8/9 Soundings to Weather Forecasting and Nowcasting. *Bull. Amer. Meteor. Soc*., **79**, 2059-2077.

Miller, A.J., L.E. Flynn, S.M. Hollandsworth, J.J. DeLuisi, I.V. Petropavlovskikh, G.C. Tiao, G.C. Reinsel, D.J. Wuebbles, J. Kerr, R.M. Nagatani, L. Bishop, and C.H. Jackman, 1997: Information Content of Umkehr and SBUV(2) Satellite Data for Ozone Trends and Solar Responses in the Stratosphere. *J. Geophys. Res*., **102**, 19,257-19,263.

NWS, cited 2006: NCEP Anomaly Correlations. [Available online from http://wwwt.emc.ncep.noaa.gov/gmb/STATS/STATS.html .]

NOAA, cited 2000: NOAA KLM Users Guide, September 2000 revision. [Available online from http://www2.ncdc.noaa.gov/docs/klm/cover.htm .]

_____, cited 2005: NOAA Polar Orbiter Data (POD) User's Guide, November 1998 revision. [Available online from http://www2.ncdc.noaa.gov/docs/klm/html/c3/sec3-3.htm **.]**

Smith, W. L., H. M. Woolf, C. M. Hayden, D. Q. Wark, and L. M. McMillin, 1979: The TIROS-N Operational Vertical Sounder. *Bull. Amer. Meteor. Soc*., **60**, 1177-1187.

Spencer, R.W., and J.R. Christy, and N. C. Grody, 1990: Global Atmospheric Temperature Monitoring with Satellite Microwave Measurements: Method and Results. *J. Climate*, **3**, 1111-1128.

Yu, T.-W., and R. D. McPherson, 1984: Global Data Assimilation Experiments with Scatterometer Winds from Seasat-A. *Mon. Wea. Rev.*, **112**, 368-376.

Zapotocny, T., W. P. Menzel, J. A. Jung, and J. P. Nelson III, 2005: A Four Season Impact Study of Rawinsonde, GOES and POES Data in the Eta Data Assimilation System. Part I: The Total Contribution. *Wea. Forecasting*, **20**, 161-177.

Zapotocny, T., J. A. Jung, J. F. Le Marshall and Treadon, R. 2007: A Two-Season Impact Study of Satellite and In Situ data I the NCEP Global Data Assimilation System. *Wea. Forecasting*, **22**, 887-909.